Construction of Evolutionary Tree for Morphological Engineering of Nanoparticles

Kwonnam Sohn,[†] Franklin Kim,[†] Ken C. Pradel,[†] Jinsong Wu,[†] Yong Peng,[‡] Feimeng Zhou,[‡] and Jiaxing Huang[†,*]

[†]Department of Materials Science and Engineering, Northwestern University, Evanston, Illinois 60208-3108, and [‡]Department of Chemistry and Biochemistry, California State University, Los Angeles, California 90032

ABSTRACT In addition to chemical composition, the chemistry of nanocrystals involves an extra structural factor—morphology—since many of their properties are size- and shape-dependent. Although often described as artificial atoms or molecules, the morphological control of nanoparticles has not advanced to a level comparable to organic total synthesis, where complex molecular structures can be rationally designed and prepared through stepwise reactions. Here we report a morphological engineering approach for gold nanoparticles by constructing an evolutionary tree consisting of a few branches of independent growth pathways. Each branch yields a string of evolving, continuously tunable morphologies from one reaction, therefore collectively producing a library of nanoparticles with minimal changes of reaction parameters. In addition, the tree also provides ground rules for designing new morphologies through crossing over different pathways.

KEYWORDS: evolutionary tree · gold nanoparticle · overgrowth · nanorod

Nanoparticles are often described as artificial atoms or molecules to construct matter. Unlike atoms or molecules, the chemistry of nanoparticles is concerned with not only their composition but also morphological factors such as size and shape.[1−3] For example, particles made of the same metal can have distinctly different optical[1,4,5] and catalytic[6−10] properties depending on their morphologies. Significant advances have been achieved in the synthetic chemistry of nanoparticles, and a morphological control paradigm[2,11−17] has been established, in which the nanoparticles are shaped by tuning the competitive growth of different crystallographic surfaces. This is typically achieved by altering reaction parameters such as temperature and surface binding agents. Numerous recipes are now available for producing nanoparticles of a great variety of morphologies and materials. However, to facilitate systematic investigation on the morphology−property relationship, it would be highly desirable if one reaction system can be engineered to yield as many different shapes as possible with minimal degree of parameter tuning.

In nature, growth of species is usually accompanied by evolutional changes in morphology over time until a final steady state is reached. Here we report that nanoparticle growth follows a similar pattern of morphological evolution (Figure 1). First, we discovered that multiple independent evolutionary pathways (Figure 1, colored coded branches) could be established starting from the same seed particle using the same reaction system. In each pathway, the seeds can evolve through a set of intermediate states (Figure 1, sub-branches) as the reaction progresses until a steady state shape is reached, after which the particles only grow in size. Each pathway carries a unique set of "codes" guiding the morphological transformation such as the growth direction and/or the preferred surface crystallographic orientation of the final shape. Therefore, instead of producing a single final product, each reaction readily yields a string of continuously tunable sizes and shapes without changing any reaction parameters. Then an evolutionary tree can be constructed, displaying a library of nanoparticles grown from the seeds. The tree also offers ground rules for designing new shapes. For example, crossing over different pathways can generate new morphologies carrying the codes of both branches. Anisotropically shaped gold nanorods were chosen as the starting seeds to facilitate the observation of different growth modes.

RESULTS AND DISCUSSION

Gold Nanorod Seeds. Gold nanorods were chosen as the model seed material to construct an evolutionary tree because they are one of the best-studied nanomaterials and

*Address correspondence to jiaxing-huang@northwestern.edu.

Received for review May 19, 2009 and accepted July 10, 2009.

Published online July 21, 2009.
10.1021/nn900521u CCC: $40.75

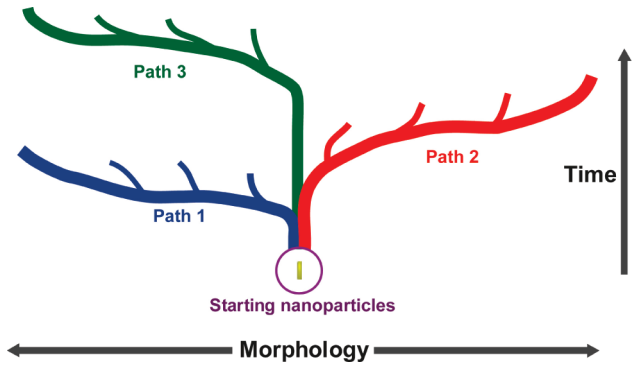

Figure 1. Evolutionary tree of nanoparticle growth. Each independent pathway should have a unique set of "codes", such as preferred growth direction and/or final surface crystallography orientation of the product, guiding the morphological evolution during nanoparticle growth. Intermediate morphologies (sub-branches) can be obtained along the progress of the reactions. Anisotropically shaped nanorods were chosen as the seeds to facilitate the observation of different growth modes.

can now be made in relatively large quantities and good uniformity.[18−22] In addition, their optical properties are sensitive to size and shape,[4,23−25] thus serving as a good marker for evolution. Gold nanorods were prepared according to the classical procedure[19,20] using gold precursor $HAuCl_4$, reducing agent ascorbic acid, and the surfactant cetyltrimethylammonium bromide (CTAB). For further growth on Au nanorods, a standard growth solution was prepared containing 2.5×10^{-4} M of $HAuCl_4$, 5.5×10^{-4} M of ascorbic acid, and 0.1 M of CTAB. The pH value of this standard growth solution was measured to be around 4. This solution is known to be metastable at room temperature. The addition of nanorods can induce *in situ* autocatalytic deposition of Au.

We have identified three independent overgrowth pathways of the nanorods using growth solutions containing the same three reagents. In the first pathway, gold nanorods preferably grow on their tips, leading to a final peanut-shaped particle. In the second pathway, the nanorods enlarge uniformly in all directions before reaching a square cuboidal final shape. In the third pathway, the nanorods preferably grow around its waist, quickly reducing its aspect ratio to 1, and finally turning into slightly truncated octahedrons. In each route, the intermediate products can be harvested along the progress of the reactions, or as the end products in reactions with reduced amount of growth solutions, thus offering continuous, fine-tuning capability of particle morphologies and, therefore, their optical properties, without changing any reaction conditions.

Evolutionary Path 1: Tip Overgrowth (Figure 2). In this tip growth pathway, the Au nanorods were added to a modified growth solution containing only 10% of CTAB as used in the standard growth solution. The pH value of such growth solution was measured to be around 4. Reactions with increasing amount of growth solution were carried out to capture the intermediate shapes. The SEM images in Figure 2 reveal the shape evolution of nanoparticles along the reaction. The starting nanorods were first transformed into dumbbell shapes (Figure 2b,c) due to preferred deposition of gold at the tips. Then they gradually turned into peanut-shaped nanoparticles (Figure 2d−h). Size analysis in Figure 2i shows the change of nanoparticles' dimension as a function of the amount of growth solution. The original Au nanorods are on average 11.2 ± 1.2 nm wide and 46.3 ± 2.8 nm long with an aspect ratio of around 4.2. During tip overgrowth, the diameter increased to 47.6 ± 5.9 nm at the center and 54.7 ± 4.1 nm at the tips, while the length increased to 114.1 ± 9.7 nm. The growth rate in the longitudinal direction is about 2-fold faster than in the transverse direction, thus decreasing the aspect ratio to around 2. The UV−vis spectra (Figure 2j) of the samples are consistent with the shape evolution seen in the SEM images and size analysis data. During the overgrowth process, the longitudinal surface plasmon band was gradually blue-shifted due to the decreased aspect ratio, while the transverse mode became red-shifted due to increased diameter and also much stronger due to enhanced scattering.[26] The final particle still has an anisotropic shape with two well-separated surface plasmon peaks. Elongated gold nanoparticles have been found useful for photothermal cancer therapy[27−30] as well as light scattering markers for rotational motions.[31,32] The continuous morphological tuning of such elongated nanoparticles makes it possible to engineer nanoparticle morphologies with the most desirable optical signatures for these applications.

Evolutionary Path 2: Isotropic Overgrowth (Figure 3). When the standard growth solution containing 0.1 M of CTAB was used, an isotropic overgrowth pathway was observed. The pH value of such growth solution was measured to around 4. Figure 3 shows the evolution of Au nanorod seeds with increasing amount of growth solution. The SEM images reveal that the starting nanorods were enlarged in all directions during growth. First they became fattened with rounded tips (Figure 3b−e) and finally turned into square cuboids with increasingly sharpened edges and points (Figure 3f−h). Square cuboids seem to be the final equilibrium shape of this pathway as the particles did not change shape further but only grew larger during later stages of the reaction. Size analysis data in Figure 3i shows the change of the nanoparticle dimension as a function of the amount of growth solution. The original Au nanorods are 14.9 ± 1.7 nm wide and 55.2 ± 5.5 nm long on average with an aspect ratio of around 3.8. During the isotropic overgrowth, the width increased to 66.8 ± 7.0 nm and the length increased to 124.7 ± 5.8 nm. The growth rate in the longitudinal and transverse directions are comparable. The aspect ratios of the products also gradually decreased, reaching a final value of around 2.0. UV−vis spectra (Figure 3j) of the samples are consistent with

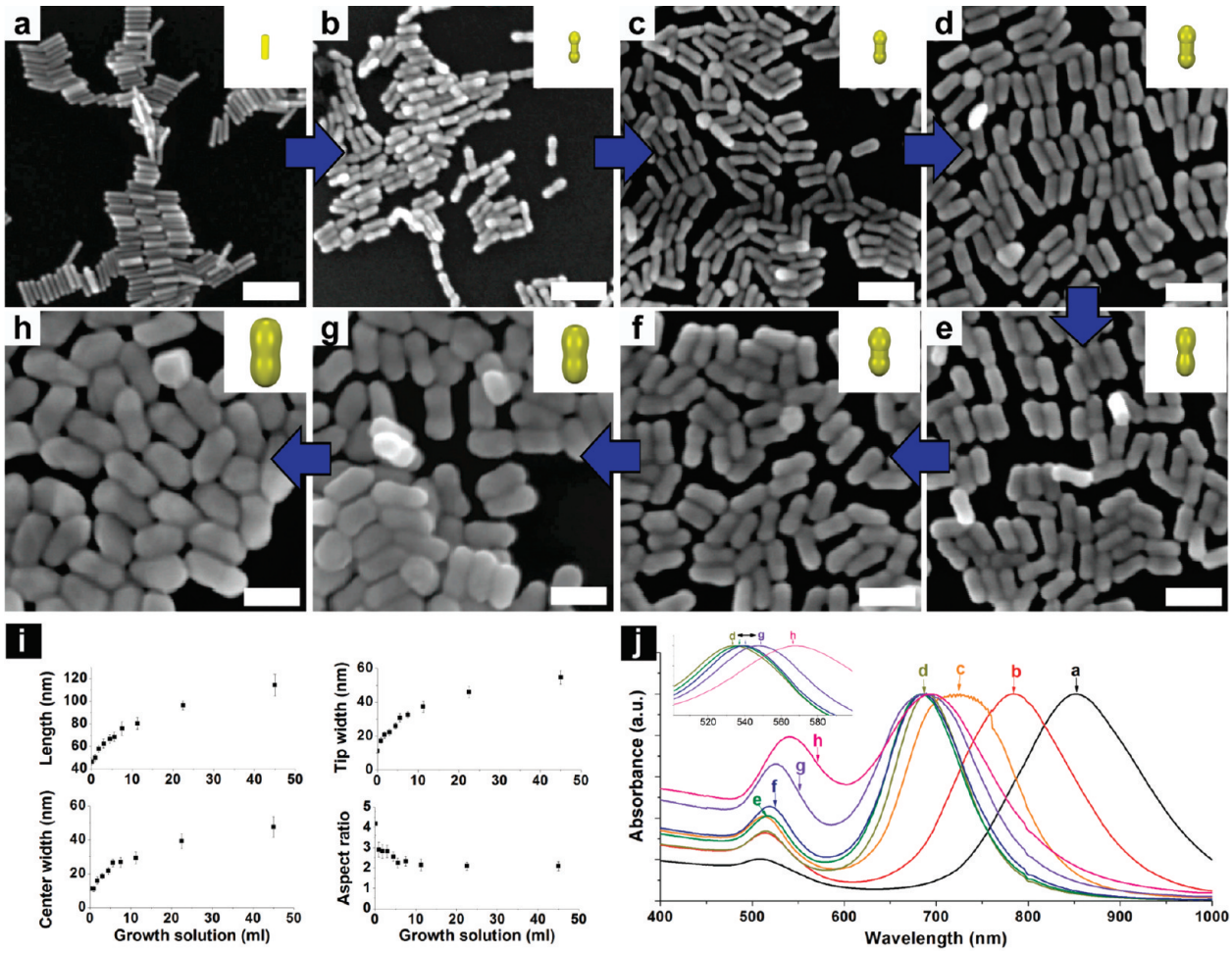

Figure 2. Evolutionary path 1: Tip overgrowth on Au nanorods using a growth solution containing less than standard CTAB concentration (0.01 M), ascorbic acid, and $HAuCl_4$ (pH ~4). (a−h) SEM images showing the morphological evolution of nanoparticles from (a) rods, to (b,c) dumbbells, to the final (d−h) peanut shape using increasing volume of growth solutions of 0.9, 1.8, 4.5, 7.5, 11.25, 22.5, to 45 mL, respectively. The insets show geometrical models of the corresponding shapes. (i) Size analysis of the products showing the changes in length, tip width, center width, and aspect ratio (length *versus* tip width) as a function of the amount of growth solution. The growth rates in the longitudinal direction were around twice as along the transverse direction. The aspect ratios of the products gradually decreased, reaching a final value of around 2.0. (j) Normalized UV−vis spectra of the samples are consistent with the shape evolution seen in the SEM images. Longitudinal plasmon bands are present in all of the spectra since the aspect ratios of the particles were persistently greater than 1 (d−h, and the magnified view in the inset). All scale bars in a−h represent 100 nm.

the morphological evolution seen in the SEM images and size analysis data. During the overgrowth process, the longitudinal surface plasmon band was gradually blue-shifted, while the transverse mode was red-shifted and intensified as well, finally merging with the longitudinal mode. The final square cuboids are dominantly bound by {100} surfaces as shown in the electron diffraction pattern (Figure S1c in the Supporting Information).

Evolutionary Path 3: Anisotropic Overgrowth (Figure 4). An anisotropic shape evolution pathway was identified when the nanorod seeds were grown in a modified, acidic growth solution with 0.05 M of CTAB. The pH value of such growth solution was adjusted to around 1 by a mineral acid such as HCl or HNO_3. Figure 4 shows the evolutionary change of Au nanorod seeds with increasing amount of growth solution. The starting nanorods first preferably grew in their transverse direction, turning into fattened nanorods with sharpening tips (Figure 4b−d). Then they transformed into steady state shape of slightly truncated octahedron (Figure 4e−h) and only grew larger afterward. Size analysis (Figure 4i) shows that the initial growth rate along the width was much faster than along the length direction. Therefore, the aspect ratio of the nanoparticles quickly decreased to 1 when they became octahedrons. After that, the shape remained the same during further growth, keeping the aspect ratio as 1. Since the particles lost anisotropy, the growth rate then became isotropic. UV−vis spectra of the intermediate products are consistent with the shape evolution seen in the SEM images. The longitudinal plasmon band is blue-shifted (Figure 4a−d) and eventually merged with the transverse mode (Figure 4e−h) due to the loss of anisotropy. The red shift of the merged surface plasmon band at shorter wavelengths (e−h, and the magnified view in the inset) is due to the enlarge-

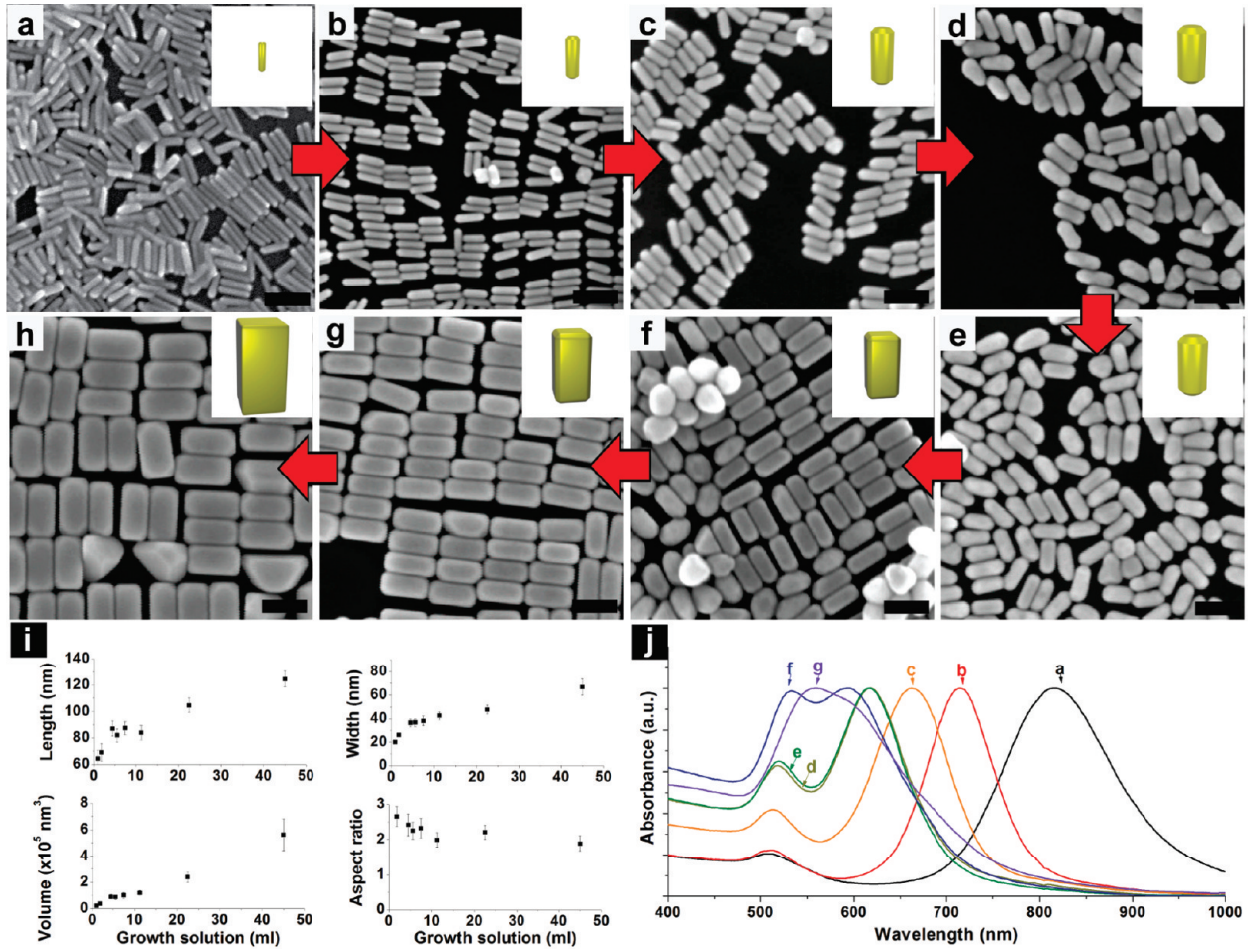

Figure 3. Evolutionary path 2: Isotropic overgrowth on Au nanorods using growth solution containing CTAB (0.1 M), ascorbic acid, and $HAuCl_4$ (pH ~4). (a−h) SEM images showing the morphological evolution of nanoparticles from (a) rods, (b−e) fattened rods to the final (f−h) square cuboids with increasingly sharpened edges and points using increasing volume of growth solutions from 0.9, 1.8, 4.5, 5.6, 11.25, 22.5, to 45 mL, respectively. The insets show geometrical models of the corresponding shapes. (i) Size analysis of the products showing the changes in length, diameter, volume, and aspect ratio as a function of the amount of growth solution. The growth rates in the transverse and longitudinal directions were comparable. The aspect ratios of the products gradually decreased, reaching a final value of around 2.0. (j) Normalized UV−vis spectra of the samples are consistent with the shape evolution seen in the SEM images. Longitudinal plasmon bands are seen in all of the spectra since the aspect ratios of the particles were persistently greater than 1. All scale bars in a−h represent 100 nm.

ment of particles. The final truncated octahedrons are dominantly bound by {111} facets as confirmed by the electron diffraction pattern (Figure S1d in the Supporting Information). The same pattern of evolution can be observed along the progress of reactions using sufficient amount of growth solutions. Figure S2 in the Supporting Information shows the intermediate products collected from a reaction using 22.5 mL of growth solution, showing the same rods-to-octahedrons transition. Although the evolution progress can be controlled by both the reaction time and the amount of growth solution, the latter is relatively easier to operate in practice. The same evolutionary pathway was also obtained using gold nanorods with different aspect ratio (Figure S3 in the Supporting Information).

Completed Evolutionary Tree. With the three independent pathways identified, namely, the isotropic overgrowth (Figure 5, red branch), the anisotropic overgrowth (Figure 5, green branch), and the tip overgrowth (Figure 5, blue branch), an evolutionary tree can now be constructed (Figure 5) starting from gold nanorod seeds. The differences in the three reactions are mainly the concentration of the surfactant CTAB and the solution pH. In general, we found that CTAB seemed to stabilize {100} facets of Au as previously reported.[33,34] Therefore, decreasing the concentration of CTAB would reduce the stabilizing effect of CTAB. The solution pH was found to be affecting the reduction rate of gold and the binding strength of CTAB to gold. At low pH (pH = 1), the gold reduction rate was significantly lowered. Quartz crystal microbalance study showed that the CTAB adsorption on gold surface was also significantly reduced (Figure S4 in the Supporting Information). Other reaction parameters such as stirring, temperature, and concentrations of $HAuCl_4$ and ascorbic acid did not seem to affect the morphological evolution pathways.

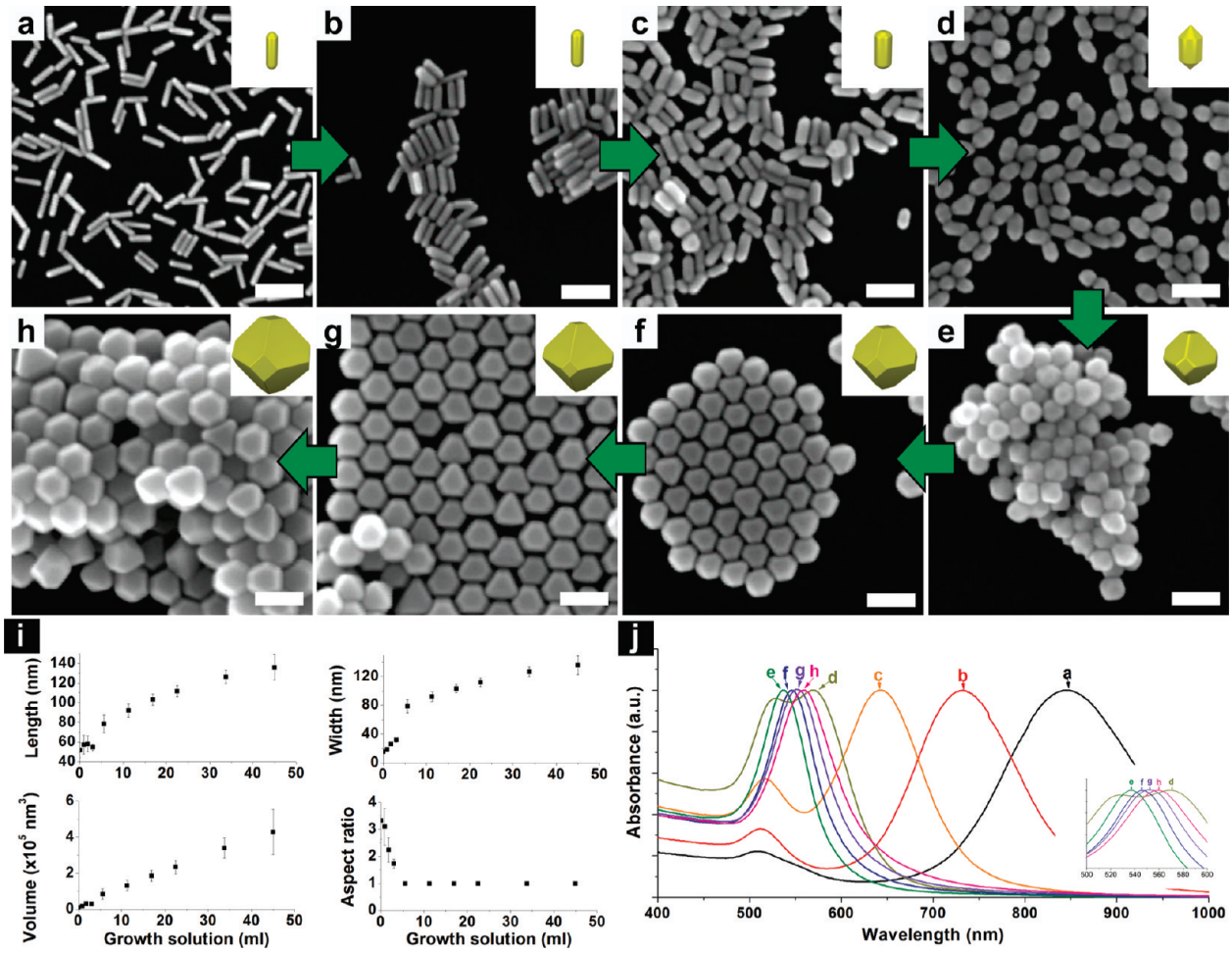

Figure 4. Evolutionary path 3: Anisotropic overgrowth on Au nanorods using growth solution with less CTAB concentration (0.05 M) and extra acid (pH ~1). (a−h) SEM images showing the morphological evolution of nanoparticles from (a) rods, (b,c) fattened rods, (d) fattened rods with sharp tips, and the final (e−h) lightly truncated octahedrons using increasing volume of growth solutions from 0.9, 1.8, 3.0, 5.6, 11.25, 16.88, to 22.5 mL, respectively. The insets show geometrical models of the corresponding shapes. (i) Size analysis of the products showing the changes in length, diameter, volume, and aspect ratio as a function of the amount of growth solution. The growth in the transverse direction was faster than along the longitudinal direction, thus quickly decreasing the particle aspect ratio to 1. (j) Normalized UV−vis spectra of the products are consistent with the shape evolution observed in the SEM images. The blue shift (a−d) and the disappearance (e−h) of the longitudinal plasmon band at longer wavelengths are due to decreased particle aspect ratio. The red shift of the single surface plasmon band at lower wavelengths (d−h, and the magnified view in the inset) is consistent with the enlargement of the particles. All scale bars in a−h represent 100 nm.

In the isotropic overgrowth route, the standard growth solution was used. The nanorods enlarged uniformly in all directions and eventually turned into a {100} bound square cuboidal shape. This is consistent with previous observations that 0.1 M CTAB can stabilize the {100} surface of gold.[33,34] The standard growth solution is slightly acidic with a pH value of around 4 due to the gold precursor and ascorbic acid. The reduction of gold precursor was quite fast under this pH. The transition from rods to square cuboids (Figure 3f−h) typically takes only a few minutes. The gold reduction rate can be significantly lowered in the presence of extra acids.[35] In the anisotropic overgrowth route, the pH of growth solution is reduced to 1. It usually takes a few hours for the nanorods to grow into the equilibrium end shape. Binding strength of CTAB to the {100} facets is also likely weakened as indicated by the QCM study (Figure S4 in the Supporting Information). Therefore, the end shapes in acidic growth solution tend to develop an increasing fraction of {111} facets when the pH is lowered (Supporting Information Figure S5). The stabilizing power of CTAB on the {100} surface can be further reduced by decreasing its concentration, making the {111} facets the most stabilized surface. Therefore, truncated octahedrons become the equilibrium end shape when the growth solution has less CTAB (0.05 M) and extra acid (pH ~1) (Figure 4). The reduced reaction speed allows sufficient time for preferred development of {111} facets on the growing nanorods, resulting in anisotropic growth toward octahedral shapes. The rods-to-octahedrons transition has been observed before in an organic solvent-based synthesis using polyvinylpyrrolidone (PVP) to stabilize {111} facets[36] and in a CTAB-based aqueous synthesis using thiol molecules to block the growth on the nanorod tips.[37] The green branch on the evolutionary tree (Fig-

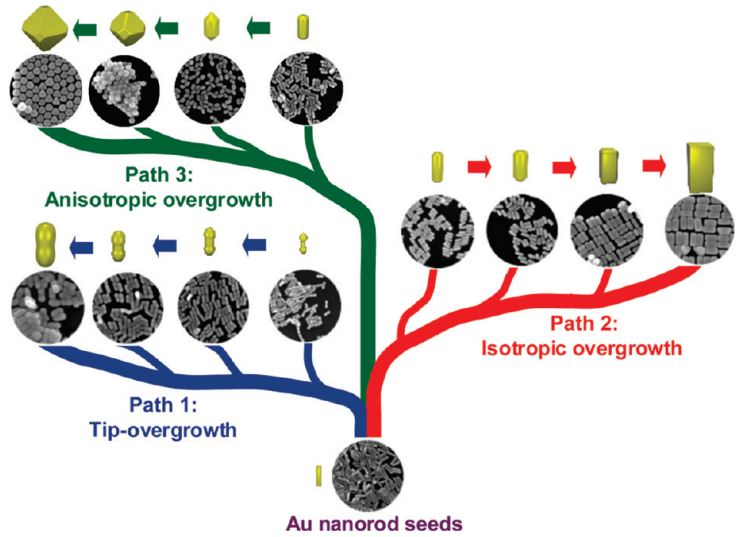

Figure 5. Completed evolutionary tree of Au nanorod overgrowth consisting of three branches. Each pathway carries a unique set of codes guiding the morphological evolution. In path 1 (blue), the nanorods preferably grow on tips and the near equilibrium final product is anisotropic and peanut-shaped. In path 2 (red), nanoparticle growth is isotropic. The seeds enlarge in all direction with comparable rate, and the surface of final product is {100} terminated. In path 3 (green), nanoparticle growth is anisotropic, thus quickly decreasing its aspect ratio to 1. The surface of final product is {111} dominated.

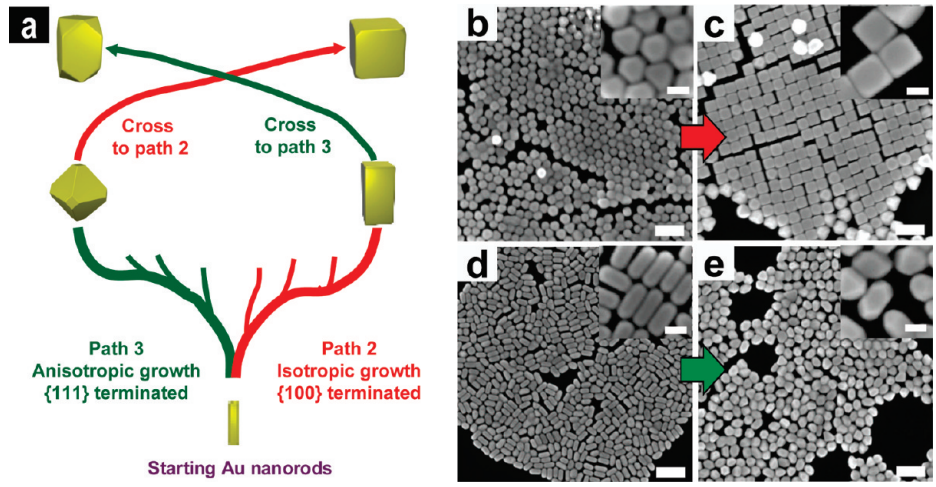

Figure 6. (a) Crossing over two evolutionary pathways can create "hybrid" morphologies carrying both sets of codes. For example, the octahedral end shapes (b) from the green pathway can growth isotropically into nanocubes (c) through an additional red evolution pathway. The nanocube products have aspect ratio of 1 and {100} terminated surfaces, which are characteristics from the green and the red pathways, respectively. When the square cuboid end products (d) from the red pathway evolve through the green pathway, they will turn into truncated square cuboids with smaller aspect ratio and more {111} surfaces, thus developing the characteristics of the green pathway. Scale bars in b−e and insets are 200 and 50 nm, respectively.

ure 5) can be obtained by adjusting solution pH and CTAB concentration without the need for introducing foreign ions (*e.g.*, when using HCl) into the reaction system. Therefore, it is a less complex reaction and better suited for constructing the tree. In the tip overgrowth route, the CTAB concentration is further reduced to 0.01 M. Therefore, the amount of CTAB bound to the seed is likely to decrease more, resulting in less ordered coverage on the tips. This would make the tips more reactive and the preferred position for gold deposition during the rapid reaction in the pH ~4 growth solution (Figure 2).

The evolutionary tree in Figure 5 thus displays three strings of gold nanoparticle morphologies from the same synthetic system with three slightly different reaction conditions. The morphologies on each string are continuously tunable by either reaction time or the amount of growth solution. Each pathway carries its own "codes" such as growth direction and/or preferred crystallographic orientation of final facets, guiding the morphological evolution. For example, the codes for the green branch would be "anisotropic growth + {111} terminated facets" and those for the red branch would be "isotropic growth + {100} terminated facets". Therefore, an evolutionary tree can offer ground rules for morphological engineering of nanoparticles. New trees can be constructed, and new nanostructures can be designed from seed particles of different shapes or even different materials.

Crossing over Different Branches. Although each pathway can already generate a collection of optically different particles, they all share the same set of codes dictating their shapes. We have found that "crossbreeding" between two different evolutionary pathways can generate new "hybrid" offspring that appear to carry a combined set of codes (Figure 6a). For example, when the truncated octahedrons (Figure 6b) from the green route were added to the growth solution used for the red route, they started to carry the red codes (isotropic growth + {100} terminated facets) and grew into a {100} terminated, isotropically shaped cube (Figure 6c). On the other hand, when the square cuboids (Figure 6d) from the red route underwent a green evolution pathway (anisotropic growth + {111} terminated facets), they grew anisotropically to decrease the aspect ratio and developed truncated {111} corners (Figure 6e). Therefore, crossbreeding can introduce more branching in the evolutionary tree. Numerous possibilities can thus be envisioned by multiple crossbreeding steps between the great varieties of morphologies on the tree.

CONCLUSION

Using nanorods as seed, we successfully constructed an evolutionary tree of gold nanoparticle growth consisting of three independent branches. Instead of generating one final shape, a single reaction now generates a string of different morphologies with unique optical signatures. The size and shape of the nanoparticles can be continuously tuned along the evolutionary pathways, leading to a library of particle morphologies with minimal need for adjusting reaction parameters. Crossing over different branches of the tree readily offers another dimension of morphological control in the library. The current three-branch tree is very likely only a portion of the crown in a much bigger evolutionary tree originating from the universal ancestor—the gold precursor $HAuCl_4$. The completion of such a comprehensive tree and the construction of evolutionary trees for other reaction systems or even different materials should eventually lead to the rational "total synthesis" of nanoparticles.

METHODS

Gold nanorod seeds were prepared by the well-known method originally developed by Murphy and El-Sayed using ascorbic acid as reducing agent and CTAB as the capping agent.[18−21] A standard growth solution for morphological evolution contains 2.5×10^{-4} M of $HAuCl_4$, 0.1 M of CTAB, and 5.5×10^{-4} M of ascorbic acid. This standard solution has a pH value of about 4. It was used for the isotropic overgrowth pathway. For the tip overgrowth path, a growth solution containing 10% concentration of the standard CTAB (0.01 M) was used. Anisotropic overgrowth was carried out in a more acidic growth solution containing 50% concentration of the standard CTAB (0.05 M). Extra acid (*e.g.*, HCl, HNO_3) was added to bring the pH down to 1. For each overgrowth route, a string of evolving morphologies can be collected either as intermediate products along the progress or as an end product of the reaction using reduced amount of growth solutions. For ease of operation, reactions with stepwise increasing amount of growth solutions were performed to capture the "snapshots" of the morphological evolution. All of the reactions were kept at 30 °C for 12 h to ensure completion. The products were collected by centrifugation and redispersed in water for spectroscopy and microscopy studies. The full experimental procedure can be found in the Supporting Information.

Acknowledgment. The work was supported by a seed grant from the Northwestern University Materials Research Science & Engineering Center (NU-MRSEC, NSF DMR-0520513). K.S. thanks the NU-MRSEC for a graduate fellowship. The electron microscopy work was performed in the EPIC facility of the NUANCE Center and the McCormick Laboratory for Manipulation and Characterization of Nano Structural Materials. F.Z. acknowledges partial support of this research by the NIH-RIMI Program at California State University—Los Angeles (P20 MD001824-01), and Y.P. thanks the China Scholarship Council for the financial support.

Supporting Information Available: Experimental details, TEM images, and electron diffraction pattern of final structures, evolution progress by reaction time, pH effect on final shapes, and shape evolution from nanorods with different aspect ratios. This material is available free of charge *via* the Internet at http://pubs.acs.org.

REFERENCES AND NOTES

1. Peng, X. G.; Manna, L.; Yang, W. D.; Wickham, J.; Scher, E.; Kadavanich, A.; Alivisatos, A. P. Shape Control of CdSe Nanocrystals. *Nature* **2000**, *404*, 59–61.
2. Sun, Y. G.; Xia, Y. N. Shape-Controlled Synthesis of Gold and Silver Nanoparticles. *Science* **2002**, *298*, 2176–2179.
3. Burda, C.; Chen, X. B.; Narayanan, R.; El-Sayed, M. A. Chemistry and Properties of Nanocrystals of Different Shapes. *Chem. Rev.* **2005**, *105*, 1025–1102.
4. El-Sayed, M. A. Some Interesting Properties of Metals Confined in Time and Nanometer Space of Different Shapes. *Acc. Chem. Res.* **2001**, *34*, 257–264.
5. Murphy, C. J.; San, T. K.; Gole, A. M.; Orendorff, C. J.; Gao, J. X.; Gou, L.; Hunyadi, S. E.; Li, T. Anisotropic Metal Nanoparticles: Synthesis, Assembly, and Optical Applications. *J. Phys. Chem. B* **2005**, *109*, 13857–13870.
6. Ahmadi, T. S.; Wang, Z. L.; Green, T. C.; Henglein, A.; ElSayed, M. A. Shape-Controlled Synthesis of Colloidal Platinum Nanoparticles. *Science* **1996**, *272*, 1924–1926.
7. Lee, H.; Habas, S. E.; Kweskin, S.; Butcher, D.; Somorjai, G. A.; Yang, P. D. Morphological Control of Catalytically Active Platinum Nanocrystals. *Angew. Chem., Int. Ed.* **2006**, *45*, 7824–7828.
8. Habas, S. E.; Lee, H.; Radmilovic, V.; Somorjai, G. A.; Yang, P. Shaping Binary Metal Nanocrystals through Epitaxial Seeded Growth. *Nat. Mater.* **2007**, *6*, 692–697.
9. Xiong, Y. J.; Wiley, B.; Xia, Y. N. Nanocrystals with Unconventional Shapes—A Class of Promising Catalysts. *Angew. Chem., Int. Ed.* **2007**, *46*, 7157–7159.
10. Peng, Z. M.; Yang, H. Designer Platinum Nanoparticles: Shape, Composition in Alloys, Nanostructure and Electrocatalytic Property. *Nano Today* **2009**, *4*, 143–164.
11. Jin, R. C.; Cao, Y. C.; Hao, E. C.; Metraux, G. S.; Schatz, G. C.; Mirkin, C. A. Controlling Anisotropic Nanoparticle Growth through Plasmon Excitation. *Nature* **2003**, *425*, 487–490.
12. Kim, F.; Connor, S.; Song, H.; Kuykendall, T.; Yang, P. D. Platonic Gold Nanocrystals. *Angew. Chem., Int. Ed.* **2004**, *43*, 3673–3677.
13. Sau, T. K.; Murphy, C. J. Room Temperature, High-Yield Synthesis of Multiple Shapes of Gold Nanoparticles in Aqueous Solution. *J. Am. Chem. Soc.* **2004**, *126*, 8648–8649.

14. Yin, Y.; Alivisatos, A. P. Colloidal Nanocrystal Synthesis and the Organic−Inorganic Interface. *Nature* **2005**, *437*, 664–670.
15. Tao, A. R.; Habas, S.; Yang, P. D. Shape Control of Colloidal Metal Nanocrystals. *Small* **2008**, *4*, 310–325.
16. Xia, Y.; Xiong, Y. J.; Lim, B.; Skrabalak, S. E. Shape-Controlled Synthesis of Metal Nanocrystals: Simple Chemistry Meets Complex Physics. *Angew. Chem., Int. Ed.* **2009**, *48*, 60–103.
17. Perez-Juste, J.; Pastoriza-Santos, I.; Liz-Marzan, L. M.; Mulvaney, P. Gold Nanorods: Synthesis, Characterization and Applications. *Coord. Chem. Rev.* **2005**, *249*, 1870–1901.
18. Busbee, B. D.; Obare, S. O.; Murphy, C. J. An Improved Synthesis of High-Aspect-Ratio Gold Nanorods. *Adv. Mater.* **2003**, *15*, 414–416.
19. Nikoobakht, B.; El-Sayed, M. A. Preparation and Growth Mechanism of Gold Nanorods (NRs) Using Seed-Mediated Growth Method. *Chem. Mater.* **2003**, *15*, 1957–1962.
20. Sau, T. K.; Murphy, C. J. Seeded High Yield Synthesis of Short Au Nanorods in Aqueous Solution. *Langmuir* **2004**, *20*, 6414–6420.
21. Gou, L. F.; Murphy, C. J. Fine-Tuning the Shape of Gold Nanorods. *Chem. Mater.* **2005**, *17*, 3668–3672.
22. Khanal, B. P.; Zubarev, E. R. Rings of Nanorods. *Angew. Chem., Int. Ed.* **2007**, *46*, 2195–2198.
23. Orendorff, C. J.; Baxter, S. C.; Goldsmith, E. C.; Murphy, C. J. Light Scattering from Gold Nanorods: Tracking Material Deformation. *Nanotechnology* **2005**, *16*, 2601–2605.
24. Kim, F.; Song, J. H.; Yang, P. D. Photochemical Synthesis of Gold Nanorods. *J. Am. Chem. Soc.* **2002**, *124*, 14316–14317.
25. Link, S.; Mohamed, M. B.; El-Sayed, M. A. Simulation of the Optical Absorption Spectra of Gold Nanorods as a Function of Their Aspect Ratio and the Effect of the Medium Dielectric Constant. *J. Phys. Chem. B* **1999**, *103*, 3073–3077.
26. Jain, P. K.; Lee, K. S.; El-Sayed, I. H.; El-Sayed, M. A. Calculated Absorption and Scattering Properties of Gold Nanoparticles of Different Size, Shape, and Composition: Applications in Biological Imaging and Biomedicine. *J. Phys. Chem. B* **2006**, *110*, 7238–7248.
27. Huang, X. H.; El-Sayed, I. H.; Qian, W.; El-Sayed, M. A. Cancer Cell Imaging and Photothermal Therapy in the Near-Infrared Region by Using Gold Nanorods. *J. Am. Chem. Soc.* **2006**, *128*, 2115–2120.
28. Huang, W. C.; Tsai, P. J.; Chen, Y. C. Functional Gold Nanoparticles as Photothermal Agents for Selective-Killing of Pathogenic Bacteria. *Nanomedicine* **2007**, *2*, 777–787.
29. Huff, T. B.; Tong, L.; Zhao, Y.; Hansen, M. N.; Cheng, J. X.; Wei, A. Hyperthermic Effects of Gold Nanorods on Tumor Cells. *Nanomedicine* **2007**, *2*, 125–132.
30. Norman, R. S.; Stone, J. W.; Gole, A.; Murphy, C. J.; Sabo-Attwood, T. L. Targeted Photothermal Lysis of the Pathogenic Bacteria, *Pseudomonas aeruginosa*, with Gold Nanorods. *Nano Lett.* **2008**, *8*, 302–306.
31. Yang, H. Single-Particle Light Scattering: Imaging and Dynamical Fluctuations in the Polarization and Spectral Response. *J. Phys. Chem. A* **2007**, *111*, 4987–4997.
32. Sonnichsen, C.; Alivisatos, A. P. Gold Nanorods as Novel Nonbleaching Plasmon-Based Orientation Sensors for Polarized Single-Particle Microscopy. *Nano Lett.* **2005**, *5*, 301–304.
33. Nikoobakht, B.; El-Sayed, M. A. Evidence for Bilayer Assembly of Cationic Surfactants on the Surface of Gold Nanorods. *Langmuir* **2001**, *17*, 6368–6374.
34. Johnson, C. J.; Dujardin, E.; Davis, S. A.; Murphy, C. J.; Mann, S. Growth and Form of Gold Nanorods Prepared by Seed-Mediated, Surfactant-Directed Synthesis. *J. Mater. Chem.* **2002**, *12*, 1765–1770.
35. Kim, F.; Sohn, K.; Wu, J. S.; Huang, J. X. Chemical Synthesis of Gold Nanowires in Acidic Solutions. *J. Am. Chem. Soc.* **2008**, *130*, 14442–14443.
36. Carbo-Argibay, E.; Rodriguez-Gonzalez, B.; Pacifico, J.; Pastoriza-Santos, I.; Perez-Juste, J.; Liz-Marzan, L. M. Chemical Sharpening of Gold Nanorods: The Rod-to-Octahedron Transition. *Angew. Chem., Int. Ed.* **2007**, *46*, 8983–8987.
37. Kou, X. S.; Zhang, S. Z.; Yang, Z.; Tsung, C. K.; Stucky, G. D.; Sun, L. D.; Wang, J. F.; Yan, C. H. Glutathione- and Cysteine-Induced Transverse Overgrowth on Gold Nanorods. *J. Am. Chem. Soc.* **2007**, *129*, 6402–6403.